„To renormalize or not to renormalize ?” in the proton-deuteron scattering calculations

- two approaches which allow to include the pp Coulomb force into pd scattering calculations
- both use screening to shorten the range of the Coulomb force

the following screening form
depends on two parameters, the screening radius R and
the power n:

$$V_c^R(r) = \frac{e^2}{r} e^{-(\frac{r}{R})^n}$$

At a given value n the pure Coulomb potential results for $R \to \infty$.

The screened Coulomb potential between 2 protons together with the strong interaction V determines the 2-body pp t-matrix via the LS equation:

$$t = V + V_c^R + (V + V_c^R) G_0 t$$

Analytical properties of screened Coulomb t-matrix, off-the-energy-shell, half-shell and on-shell have been studied in the past :

J.C.Y. Chen, A.C. Chen, in *Advances of Atomic and Molecular Physics*, edited by D.R. Bates, J. Estermann, Vol. **8** (Academic Press, New York, 1972).

J.R. Taylor, Nuovo Cimento B **23**, 313 (1974).

M.D. Semon, J.R. Taylor, Nuovo Cimento A **26**, 48 (1975).

W.F. Ford, Phys. Rev. **133**, B1616 (1964).

W.F. Ford, J. Math. Phys. **7**, 626 (1966).

The most important findings:

screening limit of $\langle \vec{p}\,'|t_c^R(E)|\vec{p}\rangle$ exists for $\frac{p'^2}{m} \neq E \neq \frac{p^2}{m}$ and coincides with the unscreened pure Coulomb force expression, which is known analytically

screening limit of the on-shell t-matrix $\langle p\hat{p}\,'|t_c^R(E=\frac{p^2}{m})|\vec{p}\rangle$ approaches the analytically known unscreened Coulomb on-shell t-matrix up to a given infinitely oscillating phase factor $\Phi_R(p)$

$\Phi_R(p) = -\eta[\ln(2pR) - \gamma/n]$ where $\gamma = 0.5772\ldots$ is the Euler number and $\eta = \frac{m_p e^2}{2p}$ the Sommerfeld parameter.

Eur. Phys. J. A **40**, 215–221 (2009) R. Skibiński[1], J. Golak[1], H. Witała[1,a], and W. Glöckle[2]

Proton-proton scattering without Coulomb force renormalization

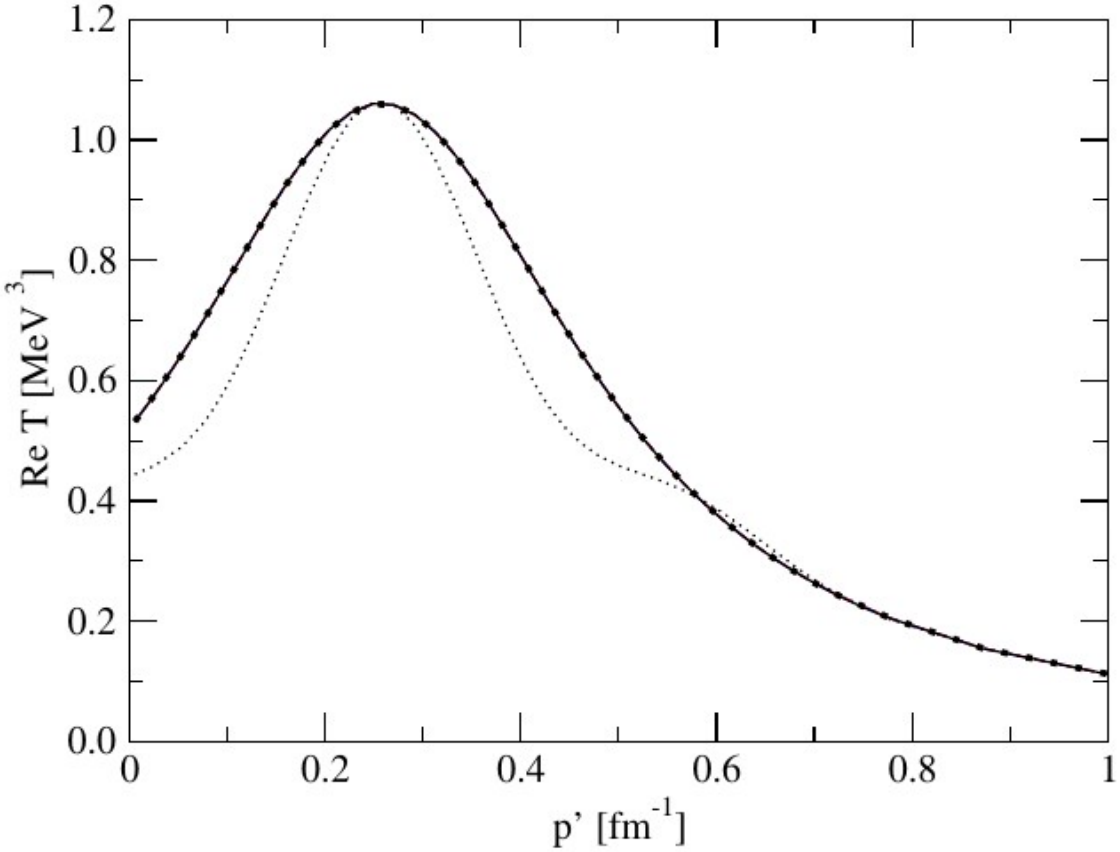

Fig. 9. (Color online) Limiting behaviour of the real part of the off-the-energy-shell screened t-matrix $t_c^R(p,p',x)$ at negative energy $E = -13\,\mathrm{MeV}$, $p = 0.36\,\mathrm{fm}^{-1}$, and $x = 0.71$, as a function of the p' momentum for $n = 4$ and different values of the screening radius R: $R = 20\,\mathrm{fm}$ (dotted line), $R = 60\,\mathrm{fm}$ (dash-dotted line), $R = 120\,\mathrm{fm}$ (dashed line), and $R = 180\,\mathrm{fm}$ (solid line). The pure Coulomb off-shell result of eq. (15) is given by thick dots.

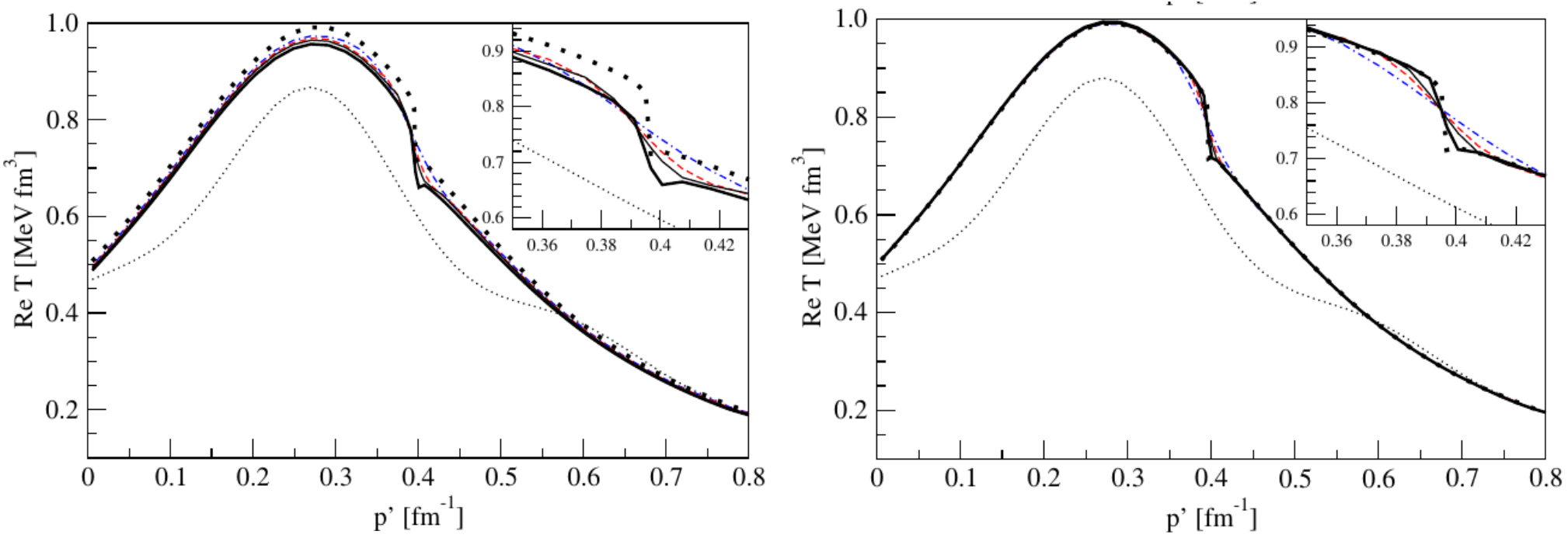

Fig. 10. (Color online) The real part of the half-the-energy-shell screened t-matrix $t_c^R(p,p,x)$ before (upper panel) and after (lower panel) the renormalization. The proton laboratory energy is $E = 13\,\mathrm{MeV}$, and $x = 0.71$. The screening potential was taken with $n = 4$ and different values of the screening radius R: $R = 20\,\mathrm{fm}$ (dotted line), $R = 60\,\mathrm{fm}$ (dash-dotted line), $R = 120\,\mathrm{fm}$ (dashed line), $R = 180\,\mathrm{fm}$ (thin solid line) and $R = 500\,\mathrm{fm}$ (thick solid line). The pure Coulomb half-shell result of eq. (17) is given by thick dots.

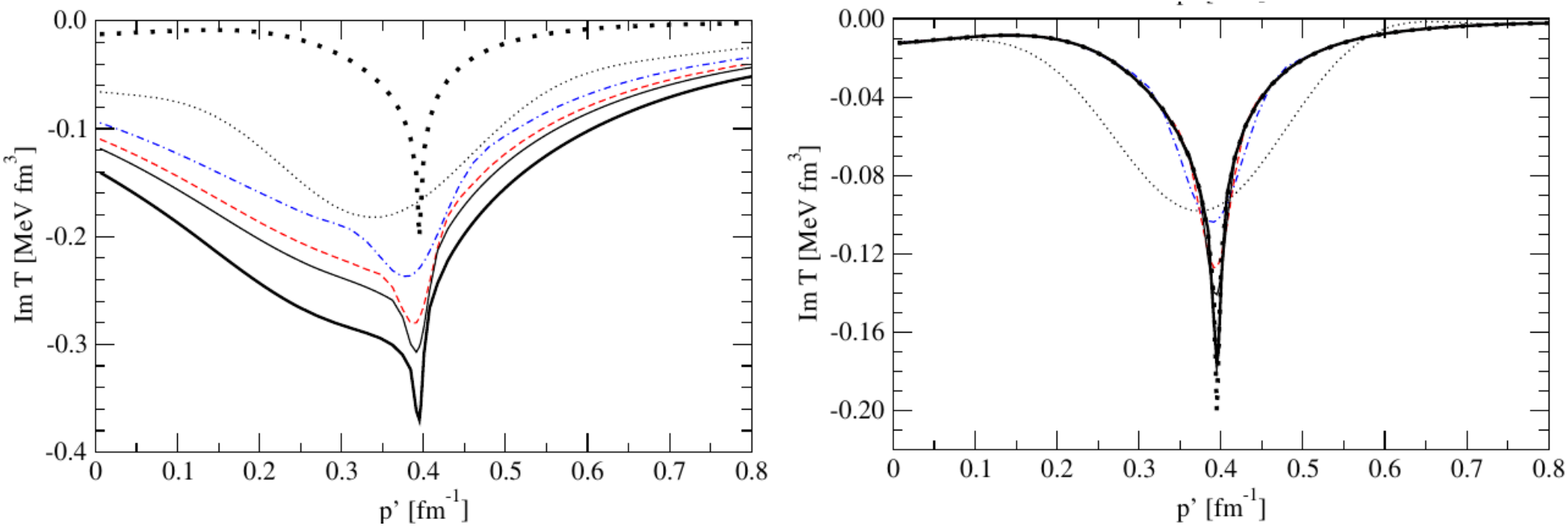

Fig. 11. (Color online) The same as in fig. 10 but for the imaginary part of the half-the-energy-shell t-matrix.

approach based on the AGS equation

A. Deltuva, A. C. Fonseca, and P. U. Sauer, Phys. Rev. C**71**, 054005 (2005).

A. Deltuva, A. C. Fonseca, and P. U. Sauer, Phys. Rev. C**72**, 054004 (2005).

$$U\,|\Phi\rangle = PG_0^{-1}\,|\Phi\rangle + PtG_0U\,|\Phi\rangle \ , \qquad (1)$$

where P is defined in terms of transposition operators, $P = P_{12}P_{23} + P_{13}P_{23}$, G_0 is the free 3N propagator and $|\Phi>$ is the initial state composed of a deuteron and a momentum eigenstate of the proton

the elastic pd scattering amplitude $< \Phi'|U|\Phi >$, with $|\Phi'>$ being the final pd state.

In our approach we use the breakup operator T defined as:

H. Witała, R. Skibiński, J. Golak, W. Glöckle, Eur. Phys. Journal A**41**, 369 (2009).

H. Witała, R. Skibiński, J. Golak, W. Glöckle, Eur. Phys. Journal A**41**, 385 (2009).

H. Witała, J. Golak, and R. Skibiński, arXiv:2310.03433 [nucl.th].

$$T = tG_0U$$

It fulfills the 3N Faddeev equation

$$T|\Phi >= tP|\Phi > +tPG_0T|\Phi > \ . \qquad (3)$$

Here the elastic scattering amplitude is calculated from solutions $T\,|\Phi\rangle$

$$\langle\Phi'|\,U\,|\Phi\rangle = \langle\Phi'|\,PG_0^{-1}\,|\Phi\rangle + \langle\Phi'|\,PT\,|\Phi\rangle$$

the transition amplitude for breakup $\langle\Phi_0|\,U_0\,|\Phi\rangle = \langle\Phi_0|\,(1+P)T\,|\Phi\rangle$

where $|\Phi_0 >= |\vec{p}\,\vec{q}\,m_1m_2m_3\nu_1\nu_2\nu_3 >$ is the state of three free outgoing nucleons.

The AGS, (1), as well as the Faddeev, (3), equations are solved in the momentum-space partial-wave basis $|pq\bar{\alpha}>$:

$$|pq\bar{\alpha}> \equiv |pq(ls)j(\lambda\frac{1}{2})I(jI)J(t\frac{1}{2})T> \quad ,$$

where one can differentiate between the partial wave states $|pq\alpha>$ with total 2N angular momentum j below some value j_{max}: $j \leq j_{max}$, in which the nuclear, V_N, as well as the pp screened Coulomb interaction, V_c^R (in isospin $t = 1$ states only), act, and the states $|pq\beta>$ with $j > j_{max}$, for which only the screened Coulomb force V_c^R is present in the pp subsystem. Incorporation of the $|pq\beta>$ states is indispensable due to the long range nature of the pp Coulomb force and the necessity to perform finally the screening limit $R \to \infty$.

The states $|pq\alpha>$ and $|pq\beta>$ form together a complete system of states (in the following we use shorthand notation $\sum_\alpha \int p^2 dp q^2 dq \, |pq\alpha\rangle \langle pq\alpha| \equiv |\alpha\rangle \langle\alpha|$):

$$\int p^2 dp q^2 dq (\sum_\alpha |pq\alpha\rangle \langle pq\alpha| + \sum_\beta |pq\beta\rangle \langle pq\beta|) = |\alpha\rangle \langle\alpha| + |\beta\rangle \langle\beta| = \mathrm{I}$$

Let us start with our approach. Projecting Eq. (3) for $T|\Phi>$ on the $|pq\alpha>$ and $|pq\beta>$ states one gets the following system of coupled integral equations

$$\begin{aligned}\langle pq\alpha|\, T\,|\Phi\rangle &= \langle pq\alpha|\, t^R_{N+c} P\,|\Phi\rangle + \langle pq\alpha|\, t^R_{N+c} P G_0|\alpha'\rangle\, \langle\alpha'|T\,|\Phi\rangle \\ &\quad + \langle pq\alpha|\, t^R_{N+c} P G_0|\beta'\rangle\, \langle\beta'|T\,|\Phi\rangle \ , \qquad (8)\\ \langle pq\beta|\, T\,|\Phi\rangle &= \langle pq\beta|\, t^R_{c} P\,|\Phi\rangle + \langle pq\beta|\, t^R_{c} P G_0\,|\alpha'\rangle\, \langle\alpha'|\, T\,|\Phi\rangle \ , \qquad (9)\end{aligned}$$

where t^R_{N+c} and t^R_c are t-matrices generated by the interactions $V_N + V^R_c$ and V^R_c, respectively.

Inserting $< pq\beta|T|\Phi >$ from (9) into (8) and using compl. relation one gets:

$$\begin{aligned}
\langle pq\alpha|\, T\,|\Phi\rangle = & \langle pq\alpha|\, t^R_{N+c} P\,|\Phi\rangle + \langle pq\alpha|\, t^R_{N+c} P G_0 t^{R3d}_c P\,|\Phi\rangle \\
& - \langle pq\alpha|\, t^R_{N+c} P G_0\,|\alpha'\rangle\,\langle\alpha'|\, t^R_c P\,|\Phi\rangle \\
& + \langle pq\alpha|\, t^R_{N+c} P G_0\,|\alpha'\rangle\,\langle\alpha'|\, T\,|\Phi\rangle \\
& + \langle pq\alpha|\, t^R_{N+c} P G_0 t^{R3d}_c P G_0\,|\alpha'\rangle\,\langle\alpha'|\, T\,|\Phi\rangle \\
& - \langle pq\alpha|\, t^R_{N+c} P G_0\,|\alpha'\rangle\,\langle\alpha'|\, t^R_c P G_0\,|\alpha''\rangle\,\langle\alpha''|\, T\,|\Phi\rangle \quad . \qquad (10)
\end{aligned}$$

This is a set of coupled integral equations in the space of the $|\alpha\rangle$ states, which exactly incorporates the contributions of the pp Coulomb interaction from all partial wave states up to infinity. It is clear that there is a price to pay for taking into account all states $|pq\beta >$: the necessity to work with the 3-dimensional Coulomb t-matrix t^{R3d}_c, obtained by solving the 3-dimensional LS equation

Presently it is practically impossible to solve Eq. (10) in its full glory. The reason are drastic amount of computer resources and of computer time required to calculate the second and the fifth terms with the 3-dimensional Coulomb t-matrix. Luckily enough, one can rather easily eliminate them at the expense of increasing the basis of $|\alpha\rangle$ states. Namely, extending the set $|\alpha\rangle$ by adding channels with higher angular momenta, in which only the pp Coulomb interaction is present, permits one to completely neglect the four terms in (10) due to their mutual cancellation: the second with the third and the fifth with the sixth term. The set (10) is then reduced to:

$$\langle pq\alpha|\, T\, |\Phi\rangle = \langle pq\alpha|\, t^R_{N+c} P\, |\Phi\rangle + \langle pq\alpha|\, t^R_{N+c} P G_0\, |\alpha'\rangle\, \langle \alpha'|\, T\, |\Phi\rangle \ , \tag{11}$$

which is a basic equation in our approach. It has identical structure as so frequently used 3N Faddeev equation for neutron-deuteron (nd) scattering

$$\langle \Phi' | \, U \, | \Phi \rangle = \langle \Phi' | \, P G_0^{-1} \, | \Phi \rangle + \langle \Phi' | \, P T \, | \Phi \rangle \quad (4)$$

To calculate in our approach the elastic scattering transition amplitude one needs in (4) the second term $\langle \vec{p}\vec{q} \, | \, T \, | \Phi \rangle$ composed of low (α) and high (β) partial wave contributions for $T|\Phi>$. Using the completeness relation (7) one gets:

$$\begin{aligned} \langle \vec{p}\vec{q} \, | \, T \, | \Phi \rangle = {} & \langle \vec{p}\vec{q} \, | \, \alpha' \, \rangle \langle \, \alpha' \, | T | \, \Phi \, \rangle + \langle \vec{p}\vec{q} \, | \, t_c^{R3d} P \, | \Phi \rangle - \langle \vec{p}\vec{q} \, | \, \alpha' \rangle \, \langle \alpha' | \, t_c^R P \, | \Phi \rangle \\ & + \langle \vec{p}\vec{q} \, | \, t_c^{R3d} P G_0 \, | \alpha' \rangle \, \langle \alpha' | \, T \, | \Phi \rangle - \langle \vec{p}\vec{q} \, | \, \alpha' \, \rangle \langle \, \alpha' \, | t_c^R P G_0 | \, \alpha'' \, \rangle \langle \, \alpha'' \, | T | \, \Phi \, \rangle \quad . \quad (12) \end{aligned}$$

To account correctly for contributions from $|\beta\rangle$ states again four terms are required, two of which contain 3-dimensional Coulomb t-matrix. The first one, $\langle \vec{p}\vec{q} \, | \, t_c^{R3d} P \, | \Phi \rangle$, corresponds to the amplitude of the Rutherford point-deuteron pd scattering and the second one, $\langle \vec{p}\vec{q} \, | \, t_c^{R3d} P G_0 \, | \alpha' \rangle \, \langle \alpha' | \, T \, | \Phi \rangle$, is a modification of the first one by nucleon-nucleon (NN) interactions.

Now we derive analogous relations in the approach based on the AGS equation. Projecting (1) on the $|pq\alpha>$ and $|pq\beta>$ states and using shorthand notation:

$$\sum_{\alpha,\tilde{\alpha}} \int p^2 dp q^2 dq p'^2 dp' \, |pq\alpha\rangle \, t^{\alpha\tilde{\alpha}}(p,p';E-\frac{3}{4m}q^2) G_0 \, \langle pq\tilde{\alpha}| \equiv |\alpha\rangle \, t^{\alpha} G_0 \, \langle\alpha|$$

one gets the following system of coupled integral equations:

$$\begin{aligned}
\langle pq\alpha| \, U \, |\Phi\rangle &= \langle pq\alpha| \, P G_0^{-1} \, |\Phi\rangle + \langle pq\alpha| \, P \, |\alpha'\rangle \, t_{N+c}^{R\alpha'} G_0 \langle\alpha'| U \, |\Phi\rangle \\
&+ \langle pq\alpha| \, P \, |\beta'\rangle \, t_c^{R\beta'} G_0 \, \langle\beta'| \, U \, |\Phi\rangle \quad , \qquad (13) \\
\langle pq\beta| \, U \, |\Phi\rangle &= \langle pq\beta| \, P G_0^{-1} \, |\Phi\rangle + \langle pq\beta| \, P \, |\alpha'\rangle \, t_{N+c}^{R\alpha'} G_0 \, \langle\alpha'| \, U \, |\Phi\rangle \\
&+ \langle pq\beta| \, P \, |\beta'\rangle \, t_c^{R\beta'} \, \langle\beta'| \, P \, |\Phi\rangle \\
&+ \langle pq\beta| \, P \, |\beta'\rangle \, t_c^{R\beta'} G_0 \, \langle\beta'| \, P \, |\alpha'\rangle \, t_{N+c}^{R\alpha'} G_0 \, \langle\alpha'| \, U \, |\Phi\rangle \quad . \qquad (14)
\end{aligned}$$

Inserting $< pq\beta|U|\Phi >$ from (14) into (13) and using (7) one gets finally:

$$\begin{aligned}\langle pq\alpha|\, U\,|\Phi\rangle = \langle pq\alpha|\, PG_0^{-1}\,|\Phi\rangle + \langle pq\alpha|\, P\,|\alpha'\rangle\, t_{N+c}^{R\alpha'} G_0 \langle\alpha'|U\,|\Phi\rangle \\ - \langle pq\alpha|\, P\,|\alpha'\rangle\, t_c^{R\alpha'}\, \langle\alpha'|\, P\,|\Phi\rangle + \langle pq\alpha|\, Pt_c^{R3d} P\,|\Phi\rangle \\ - \langle pq\alpha|\, P\,|\alpha'\rangle\, t_c^{R\alpha'} G_0 \langle\alpha'|P\,|\alpha''\rangle\, t_{N+c}^{R\alpha''} G_0 \langle\alpha''|U\,|\Phi\rangle \\ + \langle pq\alpha|\, Pt_c^{R3d} G_0 P\,|\alpha''\rangle\, t_{N+c}^{R\alpha''} G_0 \langle\alpha''|U\,|\Phi\rangle \ . \qquad (15)\end{aligned}$$

This is a set of coupled integral equations in the space spanned by the $|\alpha\rangle$ states, analogous to (12) in our approach.

Again, extending the set $|\alpha\rangle$ by adding a finite number of channels with higher angular momenta, leads to cancellations between last four terms and set (15) is reduced to the following basic equation for approach based on AGS equation [3, 4]:

$$\langle pq\alpha|\, U\,|\Phi\rangle = \langle pq\alpha|\, PG_0^{-1}\,|\Phi\rangle + \langle pq\alpha|\, P\,|\alpha'\rangle\, t_{N+c}^{R\alpha'} G_0\, \langle\alpha'|\, U\,|\Phi\rangle \ . \qquad (16)$$

To calculate the elastic scattering transition amplitude $\langle\Phi'|\,U\,|\Phi\rangle$ one needs $\langle\vec{p}\vec{q}\,|\,U\,|\Phi\rangle$ composed of low (α) and high (β) partial wave contributions for $U|\Phi>$. Employing the completeness relation (7) and Eq. (15) one gets:

$$\begin{aligned}\langle\vec{p}\vec{q}\,|\,U\,|\Phi\rangle = {} & \langle\vec{p}\vec{q}\,|\,PG_0^{-1}\,|\Phi\rangle + \langle\vec{p}\vec{q}\,|\,P\,|\alpha'\rangle\, t_{N+c}^{R\alpha'} G_0 \langle\alpha'|U\,|\Phi\rangle \\ & - \langle\vec{p}\vec{q}\,|\,P\,|\alpha'\rangle\, t_c^{R\alpha'} \langle\alpha'|P\,|\Phi\rangle + \langle\vec{p}\vec{q}\,|\,Pt_c^{R3d}P\,|\Phi\rangle \\ & - \langle\vec{p}\vec{q}\,|\,P\,|\alpha'\rangle\, t_c^{R\alpha'} G_0 \langle\alpha'|P\,|\alpha''\rangle\, t_{N+c}^{R\alpha''} G_0 \langle\alpha''|U\,|\Phi\rangle \\ & + \langle\vec{p}\vec{q}\,|\,Pt_c^{R3d}G_0P\,|\alpha''\rangle\, t_{N+c}^{R\alpha''} G_0 \langle\alpha''|U\,|\Phi\rangle \quad . \end{aligned} \tag{17}$$

$T = tG_0U \quad (2)$

Using relation (2) between U and T one finds that indeed amplitudes and thus also observables are the same in both treatments.

It should be emphasized that only by extending the set of $|\alpha\rangle$ states is it possible to neglect in (10) and (15) the terms which contain the 3-dimensional Coulomb t-matrices, and to reduce the problem in both approaches to numerically well treatable equations (11) and (16). The indication that cancellations takes place is given by convergence of predictions with respect to the total angular momentum in the two-nucleon (2N) subsystem j_{max}, which defines the set of $|\alpha\rangle$ states. It will be denoted in the following by $j_s\, j_{max}$ with j_s being the largest angular momentum in which the 2N interaction acts

It is evident that a correct treatment of the Coulomb force in both approaches requires inclusion of four additional terms in the elastic (and also breakup) transition amplitudes (the last four terms in (12) and (17)).

[2] A. Deltuva, arXiv:2311.14605v1 [nucl.th].

[3] A. Deltuva, A. C. Fonseca, and P. U. Sauer, Phys. Rev. C**71**, 054005 (2005).

[4] A. Deltuva, A. C. Fonseca, and P. U. Sauer, Phys. Rev. C**72**, 054004 (2005).

It was shown in [2] (see also [3, 4] and references therein) that in the treatment based on AGS equation (16) the elastic scattering transition amplitude acquires in the screening limit $R \to \infty$ an infinitely oscillating phase factor and must be renormalized before calculating observables. As a consequence, each term in (17) containing $U\,|\Phi\rangle$ has to be renormalized.

In our approach we solve instead of AGS the 3N Faddeev equation (11) for the $\langle pq\alpha|\,PT\,|\Phi\rangle$ states, from which later elastic scattering transition amplitude is calculated. In this way we avoid the main source of the oscillating phase factor described in [2] and the necessity of renormalization of the elastic scattering amplitude. Additionally, the structure of 3N Faddeev equation guarantees that their solutions inherit properties from the two-nucleon t-matrices providing thus an additional argument that renormalization is redundant.

the properties of t-matrices generated by the screened Coulomb force alone (in the case of partial wave decomposed t-matrices also those generated by a combination of Coulomb and nuclear parts) as well as their screening limits were studied theoretically in the past in numerous papers [11–19] and later some of these properties were confirmed numerically in [10]. The most important finding was that such off-shell t-matrices have a well defined screening limit while the half- and on-shell ones acquire in this limit an infinitely oscillating phase factor. At the same time, the elastic pd scattering amplitude gets contributions of $\langle pq\alpha| T |\Phi\rangle$ states only from the off-shell region of the Jacobi momenta magnitudes q and p in $(q-p)$ plane: $\frac{p^2}{m} + \frac{3}{4m}q^2 \neq \frac{3}{4m}q_{max}^2 = \frac{3}{4m}q_0^2 + E_d$, where m is the nucleon mass, E_d is the (negative) deuteron binding energy, and q_0 is the magnitude of the relative pd momentum. That off-shell region of $q-p$ values does not overlap with the ellipse from which half-on-shell contributions to the breakup reaction come.

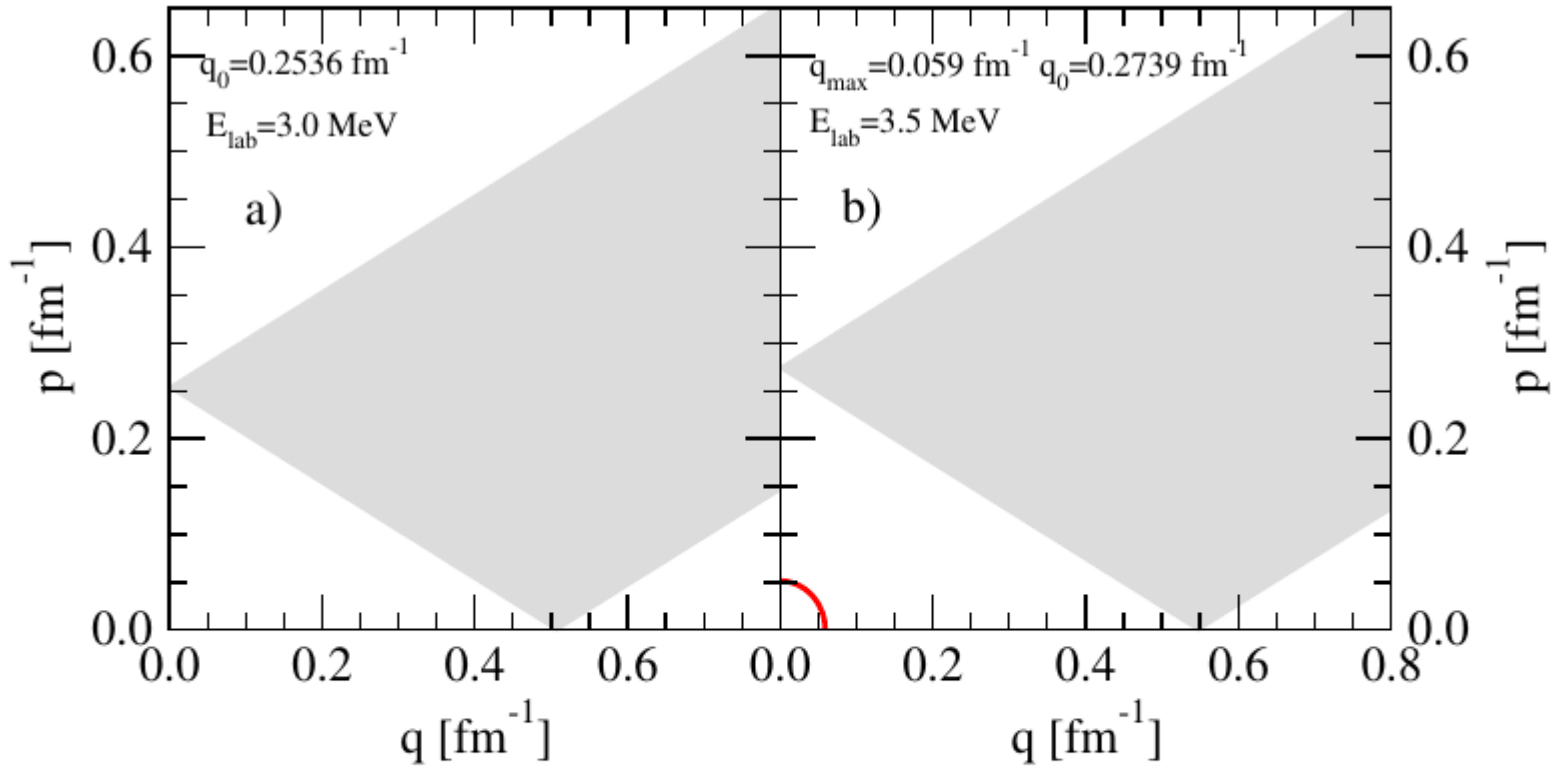

FIG. 1. (color online) Regions of the Jacobi momenta q and p values in $(q-p)$ plane which contribute to the breakup reaction ((red) solid line at $E = 3.5$ MeV, showing ellipse $\frac{p^2}{m} + \frac{3}{4m}q^2 = \frac{3}{4m}q_{max}^2 = \frac{3}{4m}q_0^2 + E_d$) and elastic scattering ($< \Phi'|PT|\Phi >$ term) (gray highlighted region) at the incoming nucleon laboratory energy $E = 3.0$ and 3.5 MeV.

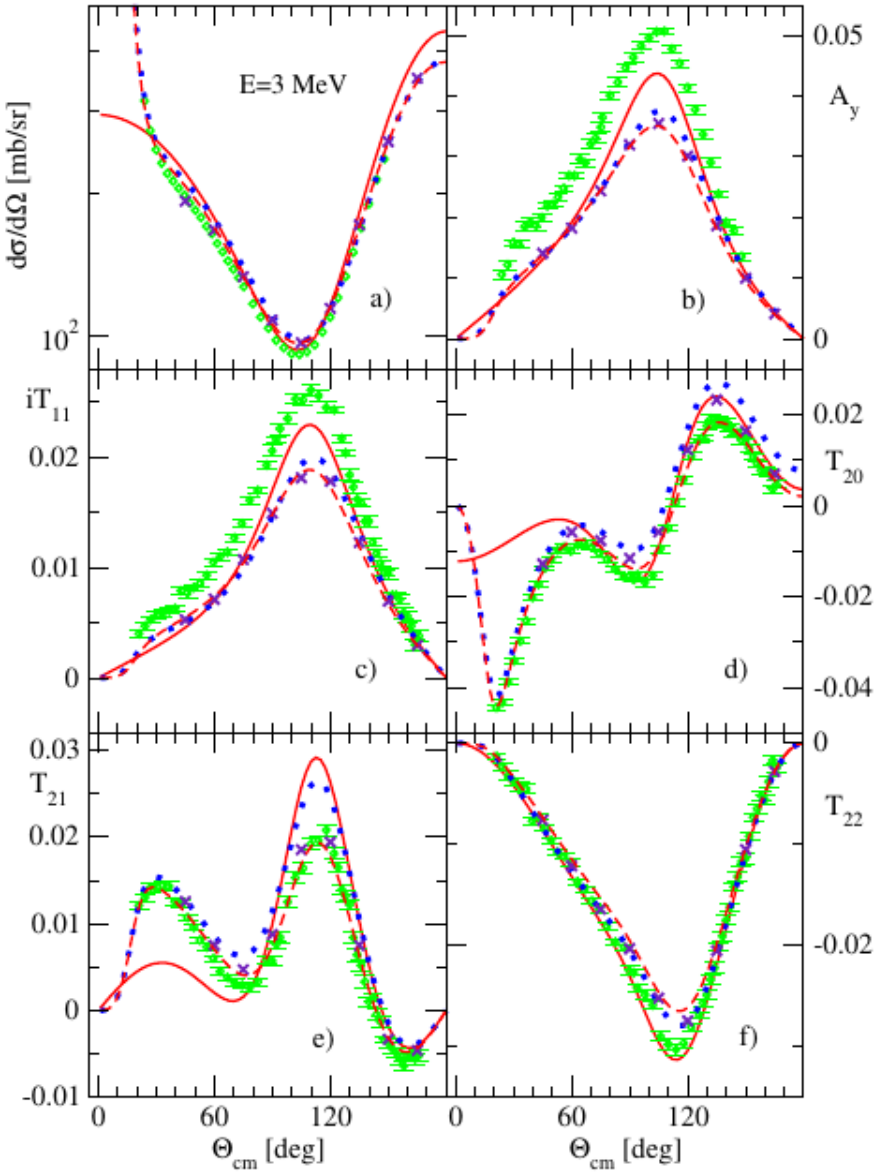

FIG. 2. (color online) Comparison of data and predictions for the pd scattering cross section $\frac{d\sigma}{d\Omega}$, proton vector A_y, deuteron vector iT_{11} and deuteron tensor T_{20}, T_{21}, T_{22} analyzing powers. They are shown as functions of a c.m. proton scattering angle Θ_{cm} and were calculated at the incoming proton laboratory energy $E = 3.0$ MeV with the approach based on Faddeev equation (11) and transition amplitude (12). The exponentialy screened Coulomb force ($R = 40$ fm, $n = 4$) and the AV18 potential [20] restricted to the $j \leq 3$ partial waves have been applied. To solve Faddeev equation the set $j_s 3j7$ of $|\alpha\rangle$ states was used. The red short dashed lines show the results when only the first three terms in (12) are taken into account. The blue dotted lines are predictions when also the fifth term in (12) ($-\langle \vec{pq} \,|\, \alpha' \rangle \langle \alpha' \left| t_c^R P G_0 \right| \alpha'' \rangle \langle \alpha'' \,|T|\, \Phi \rangle$) is included. The pure Coulomb term $\langle \Phi' | P t_c P | \Phi \rangle$ was determined using the screening limit expresion for the off-shell 3-dimensional Coulomb t-matrix (Eq. (19) in Ref. [1]). The indigo crosses show the results with all terms in (12) included. The red solid lines are predictions for nd elastic scattering and green circles represent the pd data from Ref. [21].

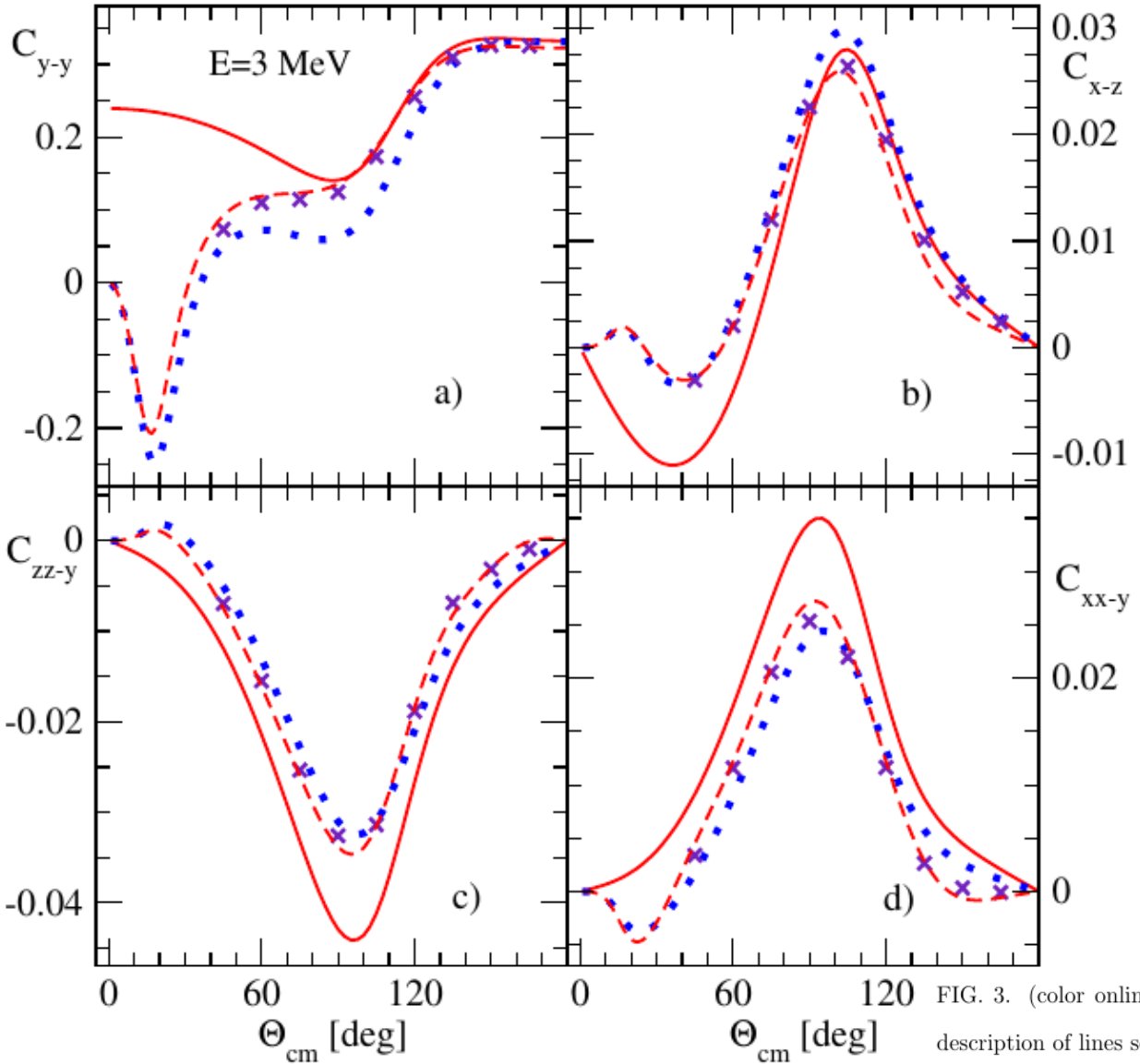

FIG. 3. (color online) The same as in Fig. 2 but for selected spin correlation coefficients. For description of lines see Fig. 2.

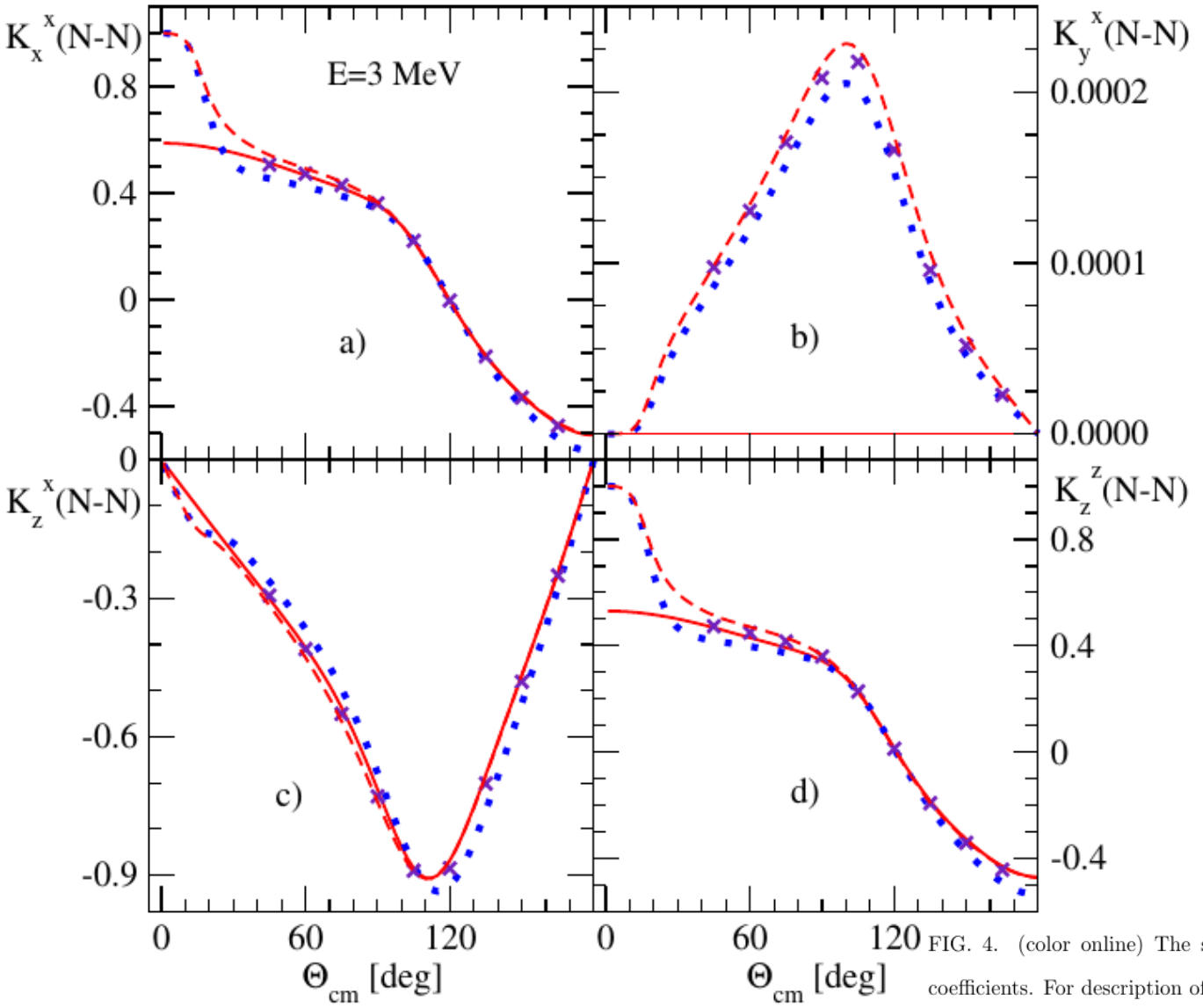

FIG. 4. (color online) The same as in Fig. 2 but for selected proton to proton spin transfer coefficients. For description of lines see Fig. 2.

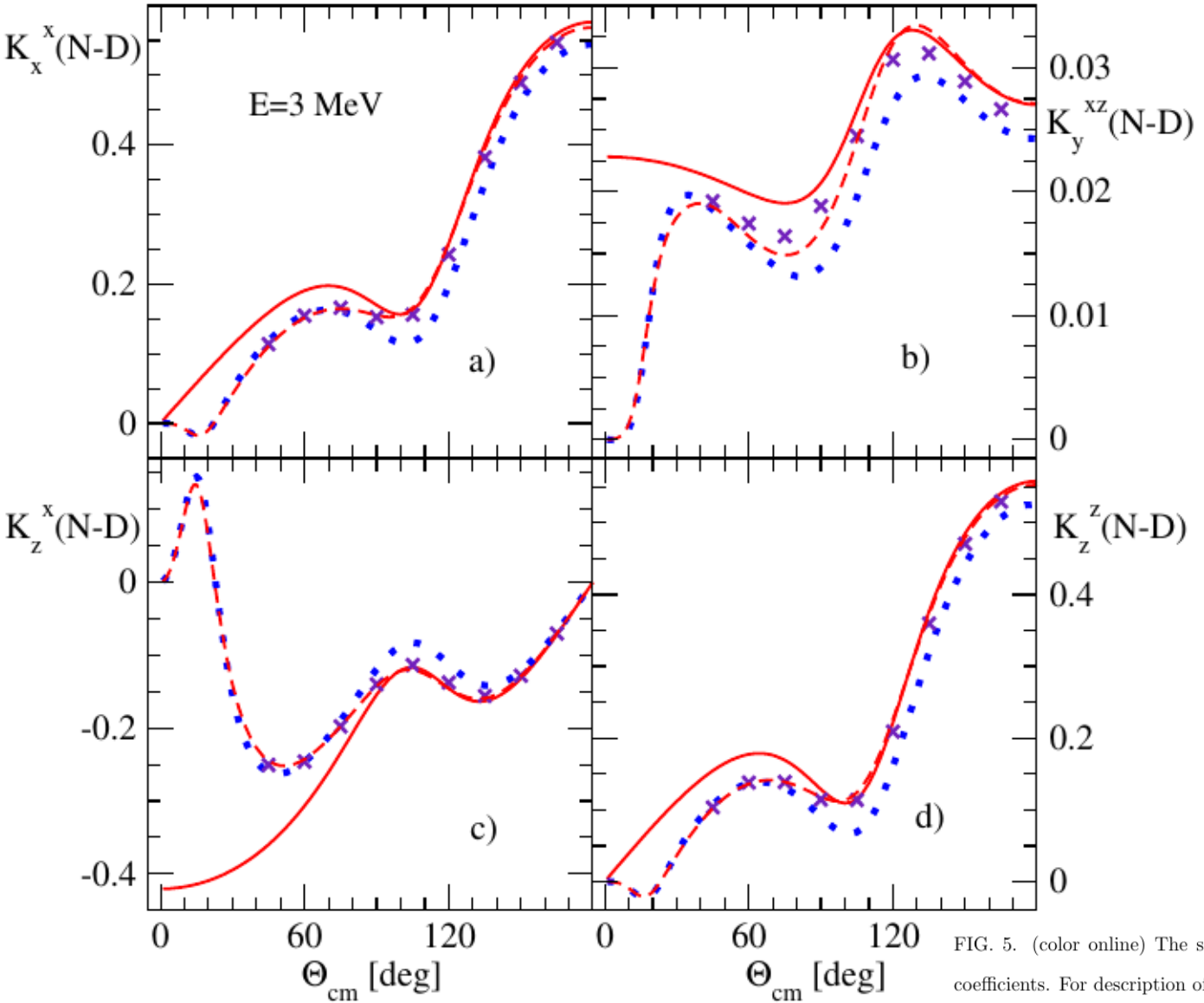

FIG. 5. (color online) The same as in Fig. 2 but for selected proton to deuteron spin transfer coefficients. For description of lines see Fig. 2.

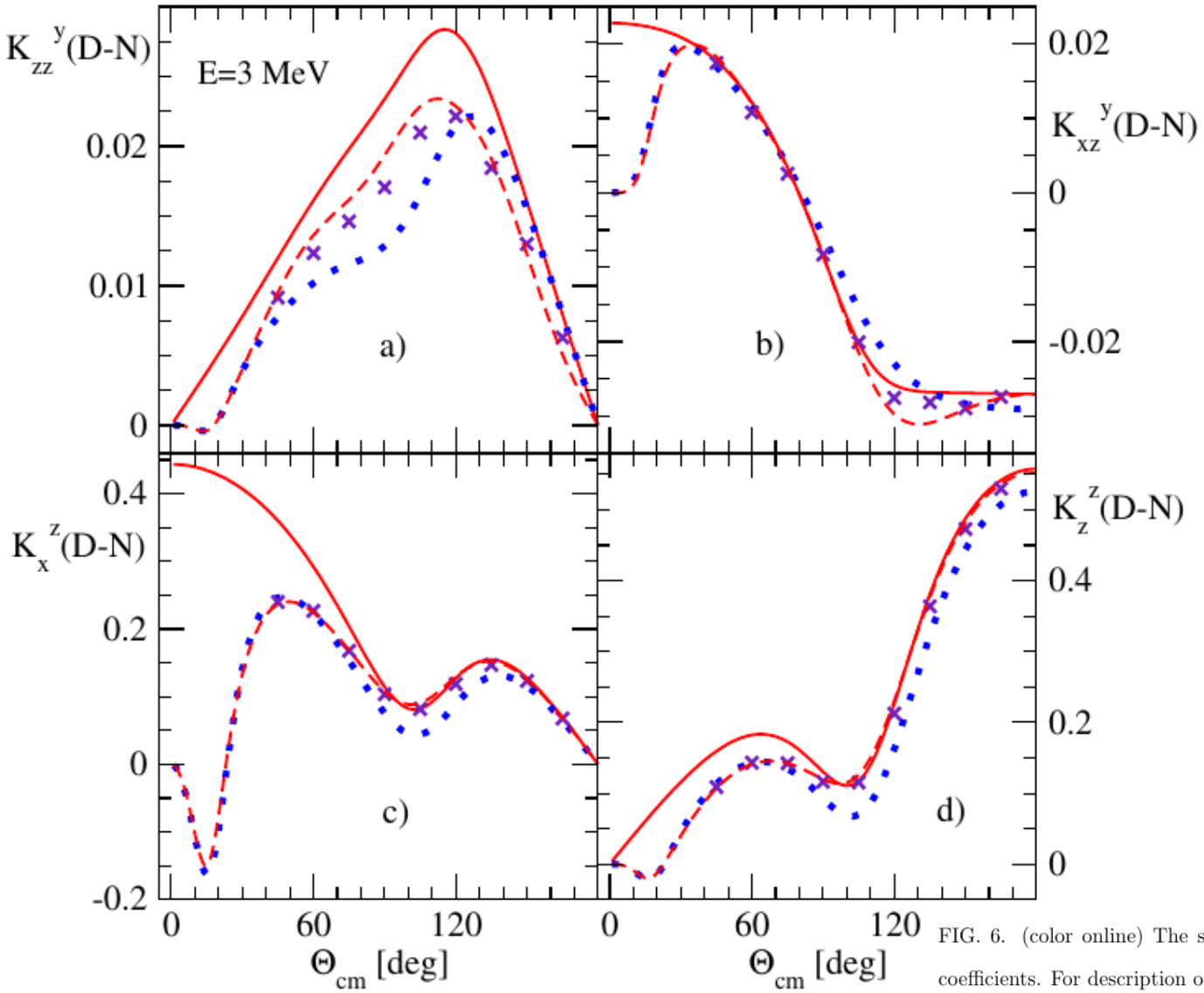

FIG. 6. (color online) The same as in Fig. 2 but for selected deuteron to proton spin transfer coefficients. For description of lines see Fig. 2.

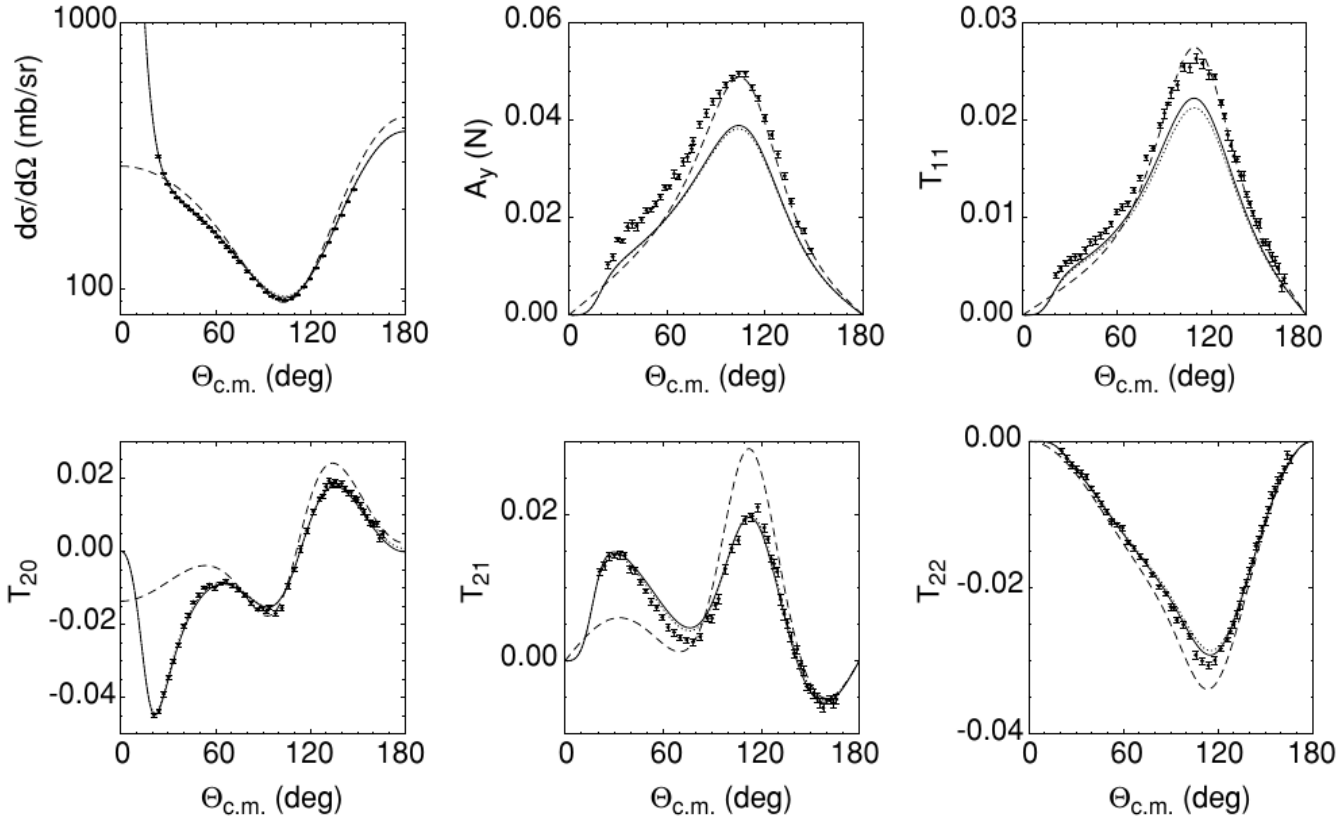

FIG. 9. Differential cross section and analyzing powers for *pd* elastic scattering at 3-MeV proton lab energy as functions of the c.m. scattering angle. Results including Δ-isobar excitation and the Coulomb interaction (solid curves) are compared to results without the Coulomb interaction (dashed curves). To better appreciate the size of the Δ-isobar effect the purely nucleonic results including the Coulomb interaction are also shown (dotted curves). The experimental data are from Ref. [22].

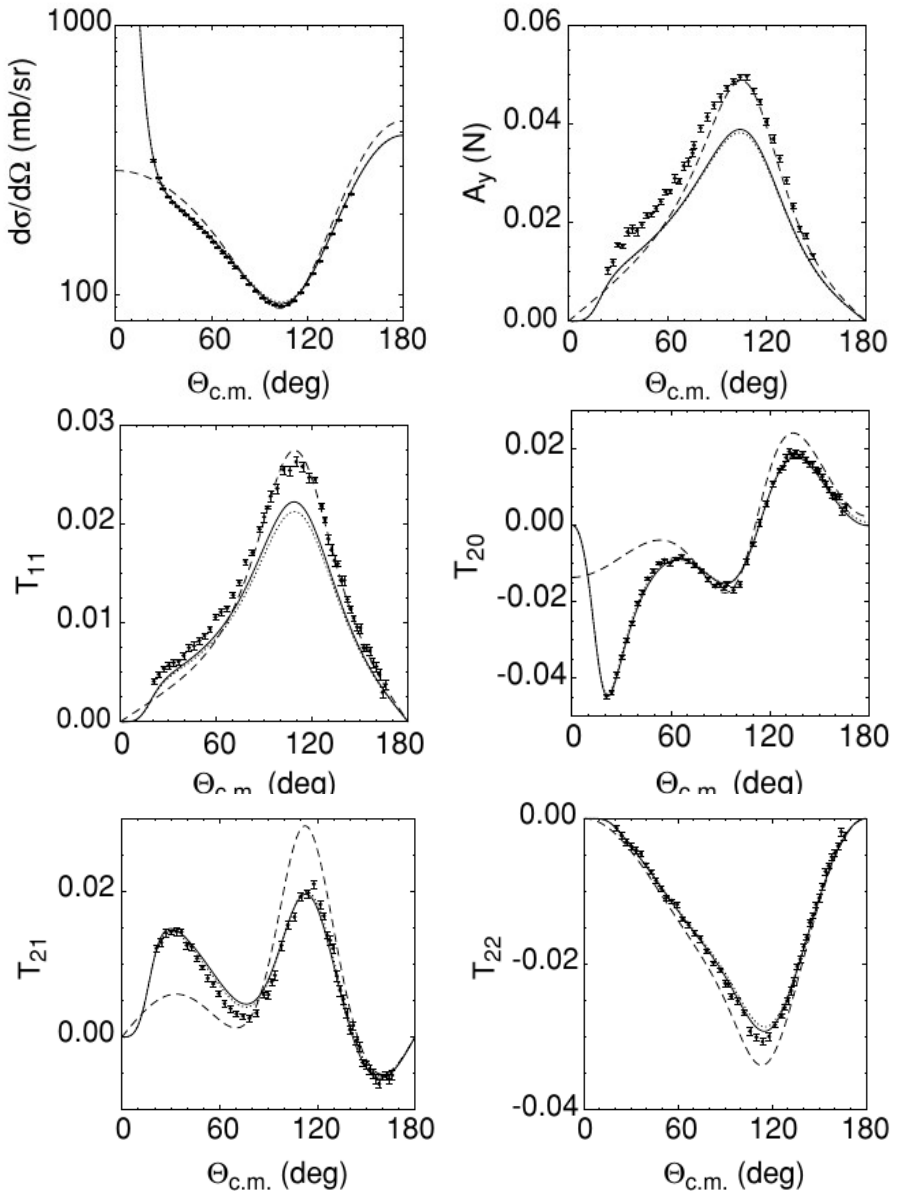
dσ/dΩ (mb/sr)
1000
100
0
60
120
180
Θc.m. (deg)
Ay (N)
0.06
0.04
0.02
0.00
T11
0.03
0.02
0.01
0.00
T20
-0.02
-0.04
T21
T22

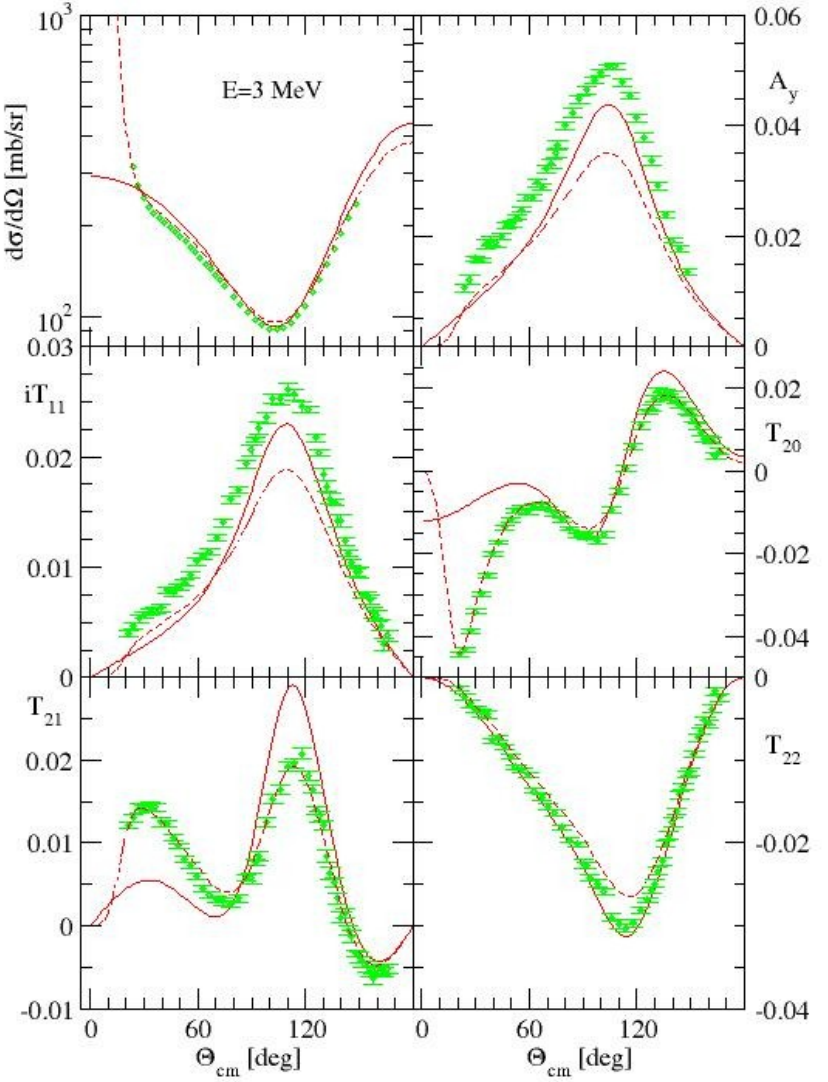
E=3 MeV
dσ/dΩ [mb/sr]
Ay
iT11
T20
T21
T22
Θcm [deg]

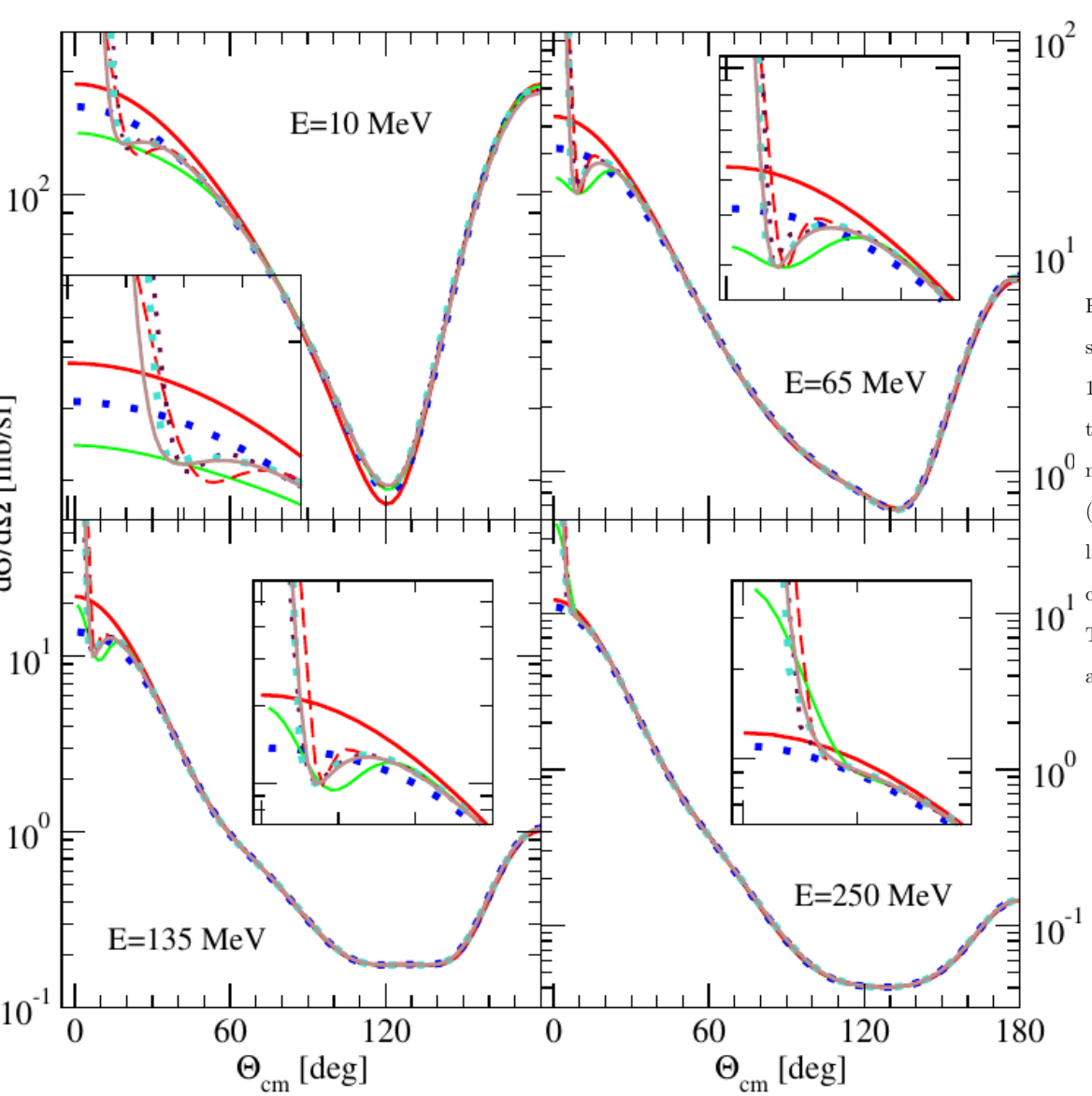

FIG. 1. (color online) The convergence in the cut-off radius R of the pd elastic scattering cross section $\frac{d\sigma}{d\Omega}$ shown as a function of the c.m. angle Θ_{cm} at the incoming lab. proton energy $E = 10, 65, 135$, and 250 MeV. These cross sections were calculated using approach based on Eq. (12), taking elastic scattering transition amplitude (16) with the screened Coulomb force and the AV18 nucleon-nucleon potential [26] restricted to the $j \leq 3$ partial waves. The screening radii are $(n = 4)$: $R = 5$ fm (blue dotted line), $R = 10$ fm (green solid line), $R = 20$ fm (red long-dashed line), $R = 30$ fm (maroon dotted line), $R = 40$ fm (turquoise dotted line). The brown solid line corresponds to the $R = 40$ fm result with the pure Coulomb term calculated according to Eq. (19). The red solid line is the nd elastic scattering cross section and the insets show the region of small angles.

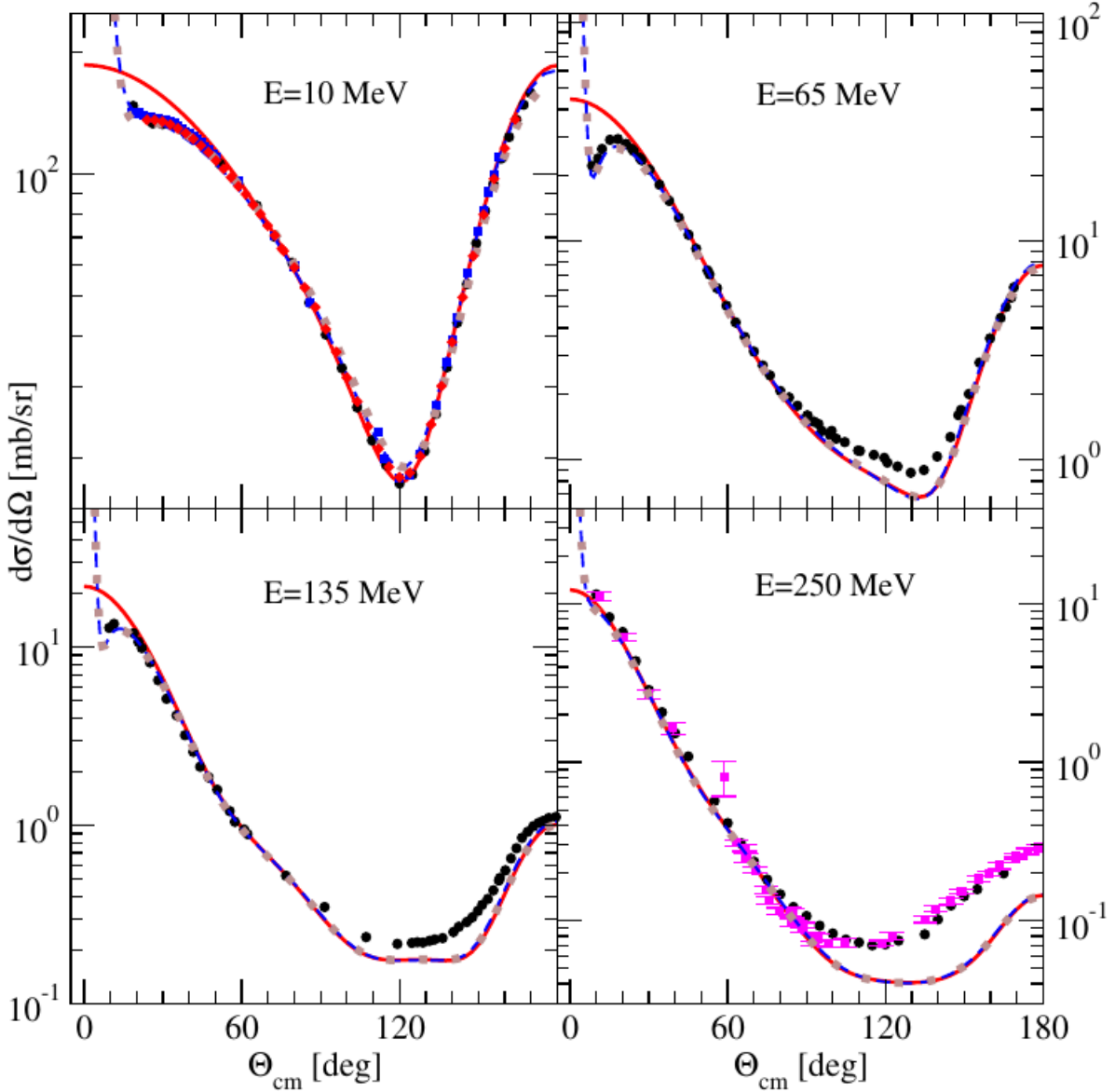

FIG. 3. Comparison of data and predictions for the pd elastic scattering cross section $\frac{d\sigma}{d\Omega}$ obtained in the approach based on Eq. (12) and using elastic scattering transition amplitude (16), at the incoming proton lab. energy $E = 10, 65, 135$, and 250 MeV. The cross sections were calculated with the screened Coulomb force ($R = 40$ fm, $n = 4$) and the AV18 nucleon-nucleon potential [26] restricted to the $j \leq 3$ partial waves. The pure Coulomb term $\langle \Phi' | P t_c P | \Phi \rangle$ was determined according to Eq. (19) (blue dashed line). At $E = 10$ MeV the set $js3j7$ of $|\alpha\rangle$-states was used while for other energies the set $js3j3$. The red solid line is the corresponding nd elastic scattering cross section. The brown dotted lines show the results when also the fourth term in (15) $(-\langle \vec{pq} \,| \sum_{\alpha'} \int |\alpha'\rangle \langle \alpha' | t_c^R P G_0 \sum_{\alpha''} \int |\alpha''\rangle \langle \alpha'' | T | \Phi \rangle)$ is included in elastic scattering transition amplitude. The black circles, blue squares and red diamonds at $E = 10$ MeV are pd elastic scattering cross section data of Ref. [31], [32], and [33], respectively. The black circles at $E = 65$ MeV are pd data from [34], at $E = 135$ MeV from [35], and at $E = 250$ MeV from [36]. The magenta squares at $E = 250$ MeV are nd data from [37].

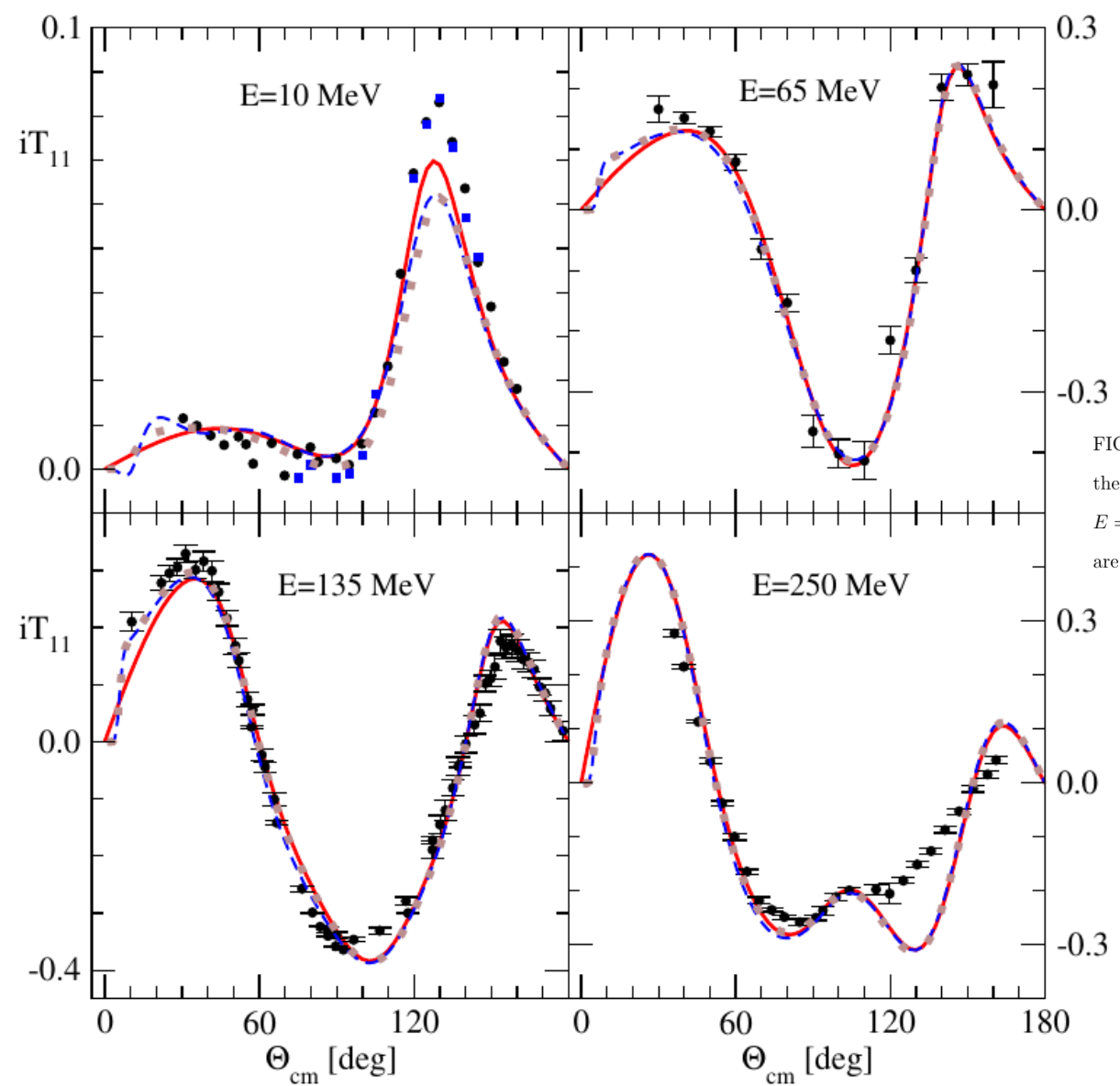

FIG. 4. (color online) The same as in Fig. 3 but for the deuteron vector analyzing power iT_{11}. For the description of lines see Fig. 3. The black circles are pd data from [38] at $E = 10$ MeV, [39] at $E = 65$ MeV, [40] at $E = 135$ MeV, and [41] at $E = 250$ MeV. The blue squares at $E = 10$ MeV are pd data from [42].

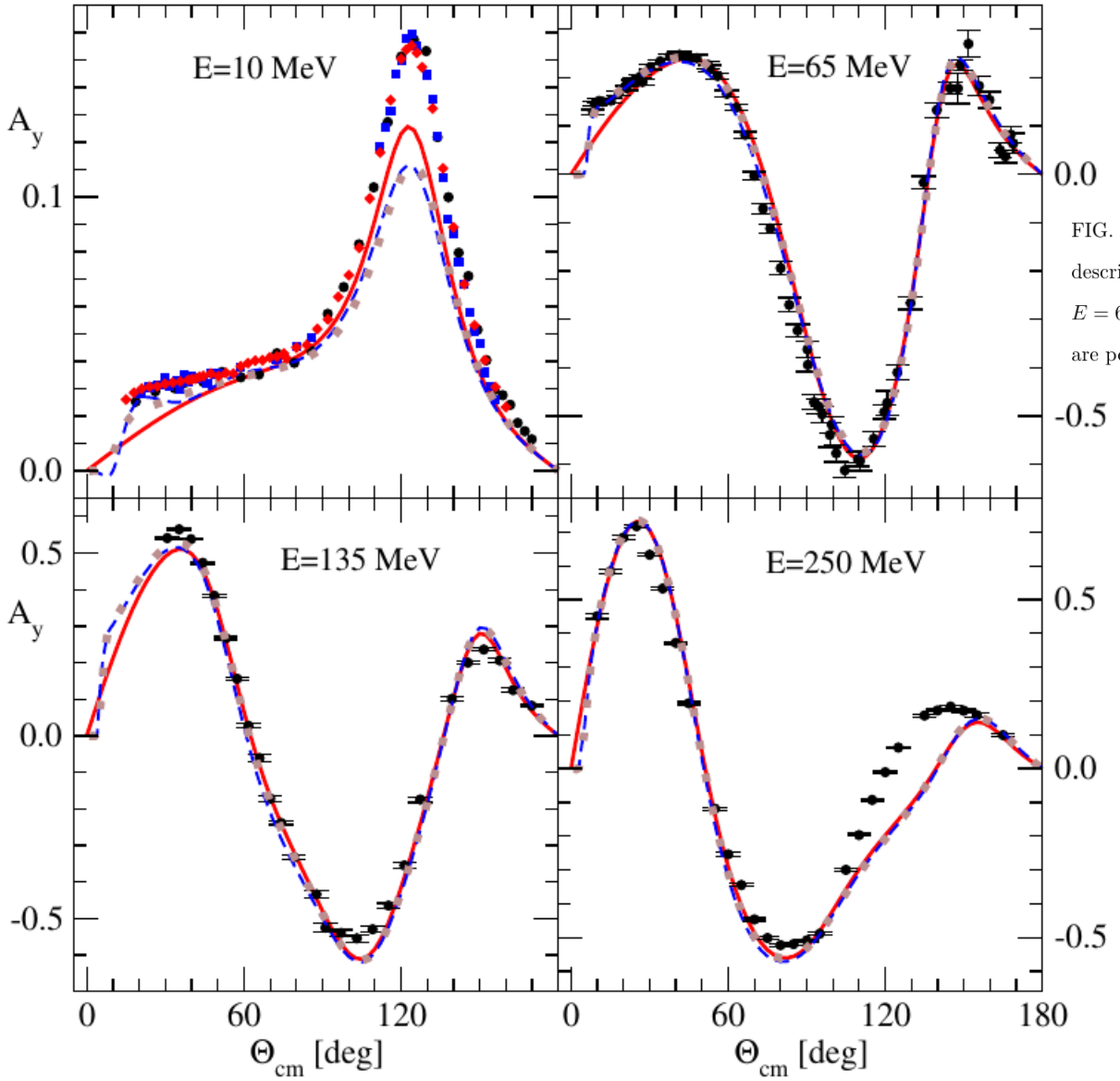

FIG. 5. (color online) The same as in Fig. 3 but for the proton analyzing power A_y. For the description of lines see Fig. 3. The black circles are pd data from [38] at $E = 10$ MeV, [34] at $E = 65$ MeV, [43] at $E = 135$ MeV, and [36] at $E = 250$ MeV. The blue squares at $E = 10$ MeV are pd data from [32] and red diamonds from [33].

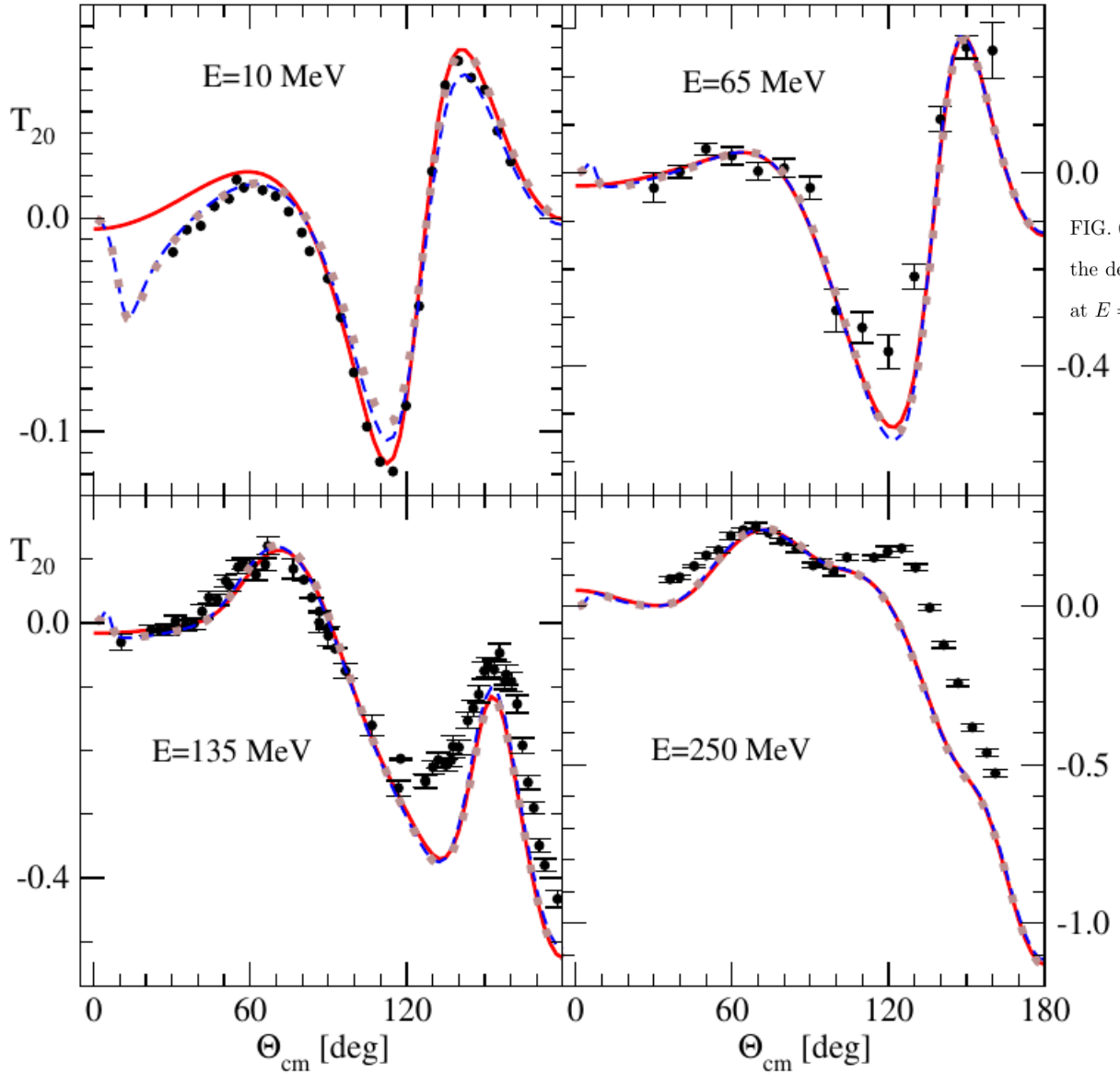

FIG. 6. (color online) The same as in Fig. 3 but for the deuteron tensor analyzing power T_{20}. For the description of lines see Fig. 3. The black circles are pd data from [42] at $E = 10$ MeV, [39] at $E = 65$ MeV, [40] at $E = 135$ MeV, and [41] at $E = 250$ MeV.

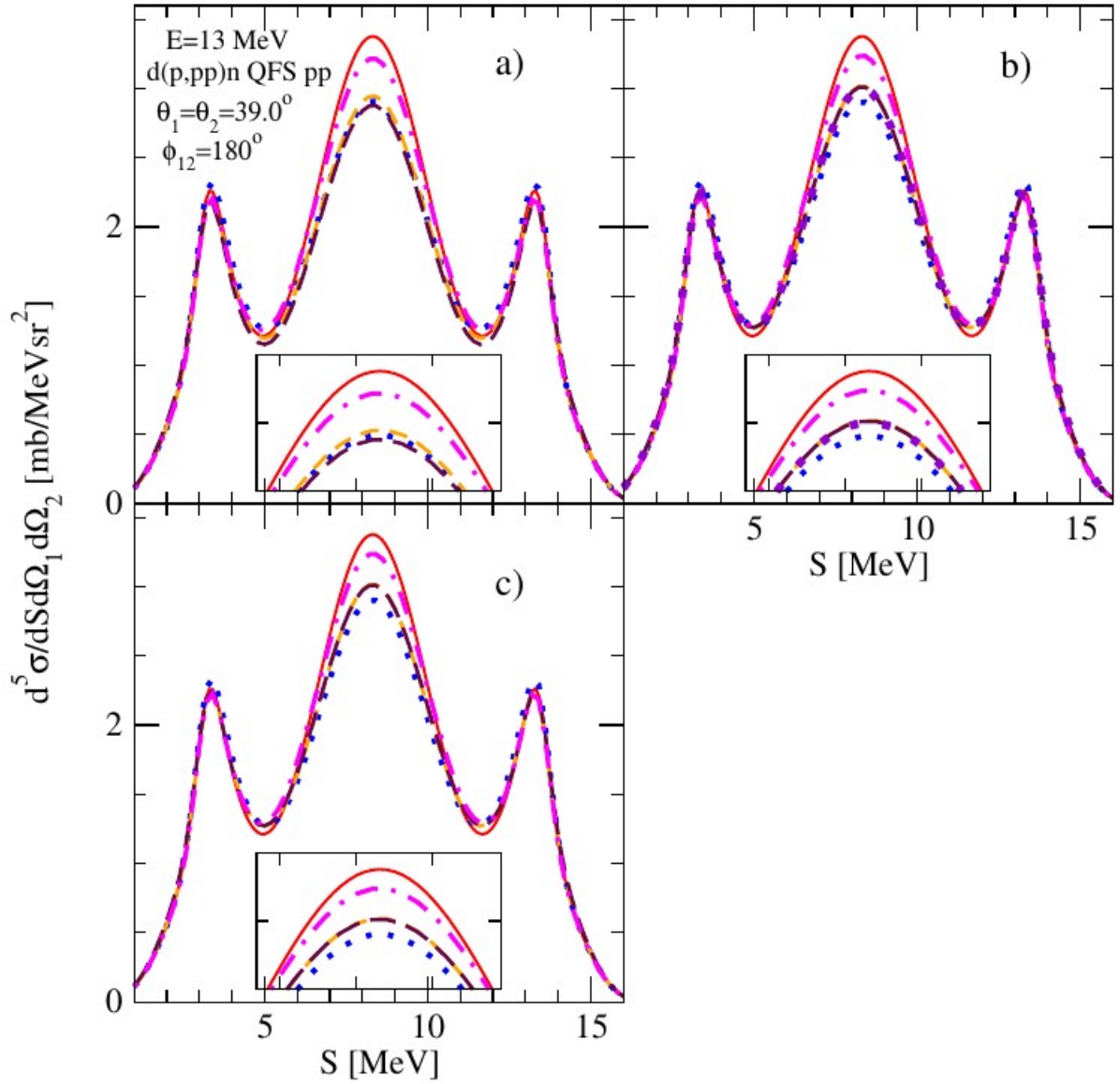

FIG. 7. (color online) The convergence with respect to the cut-off radius R of the pd breakup cross section $\frac{d^5\sigma}{d\Omega_1 d\Omega_2 dS}$ shown as a function of the S-curve length for the pp QFS kinematically complete configuration at the incoming proton lab. energy $E = 13$ MeV. The screening radii are ($n = 4$): $R = 5$ fm (blue dotted line), $R = 10$ fm (magenta dashed-dotted line), $R = 20$ fm (orange short-dashed line), $R = 40$ fm (maroon long-dashed line). These cross sections were calculated using the approach based on Eq. (12) with the screened Coulomb force and the AV18 nucleon-nucleon potential [26] restricted to the $j \leq 3$ partial waves (set $js3j3$), taking the on-shell Faddeev amplitudes obtained in two different ways and applying renormalization when calculating the breakup transition amplitude. In a) unrenormalized on-shell amplitudes gained by interpolation from the off-shell ones were used. In b) the on-shell amplitudes of a) have been renormalized before calculating observables. In c) the on-shell amplitudes were calculated according to (22) with the unrenormalized pp part of t^R_{N+c} (t^R_c) and renormalization was performed before calculating observables. The red solid line is the corresponding nd elastic scattering cross section. The violet dotted line in b) is the result with $R = 40$ fm but the pure Coulomb term $\langle \vec{p}_0 \vec{q} | (1 + P) t_c P | \Phi \rangle$ determined with the t_c of Eq. (27).

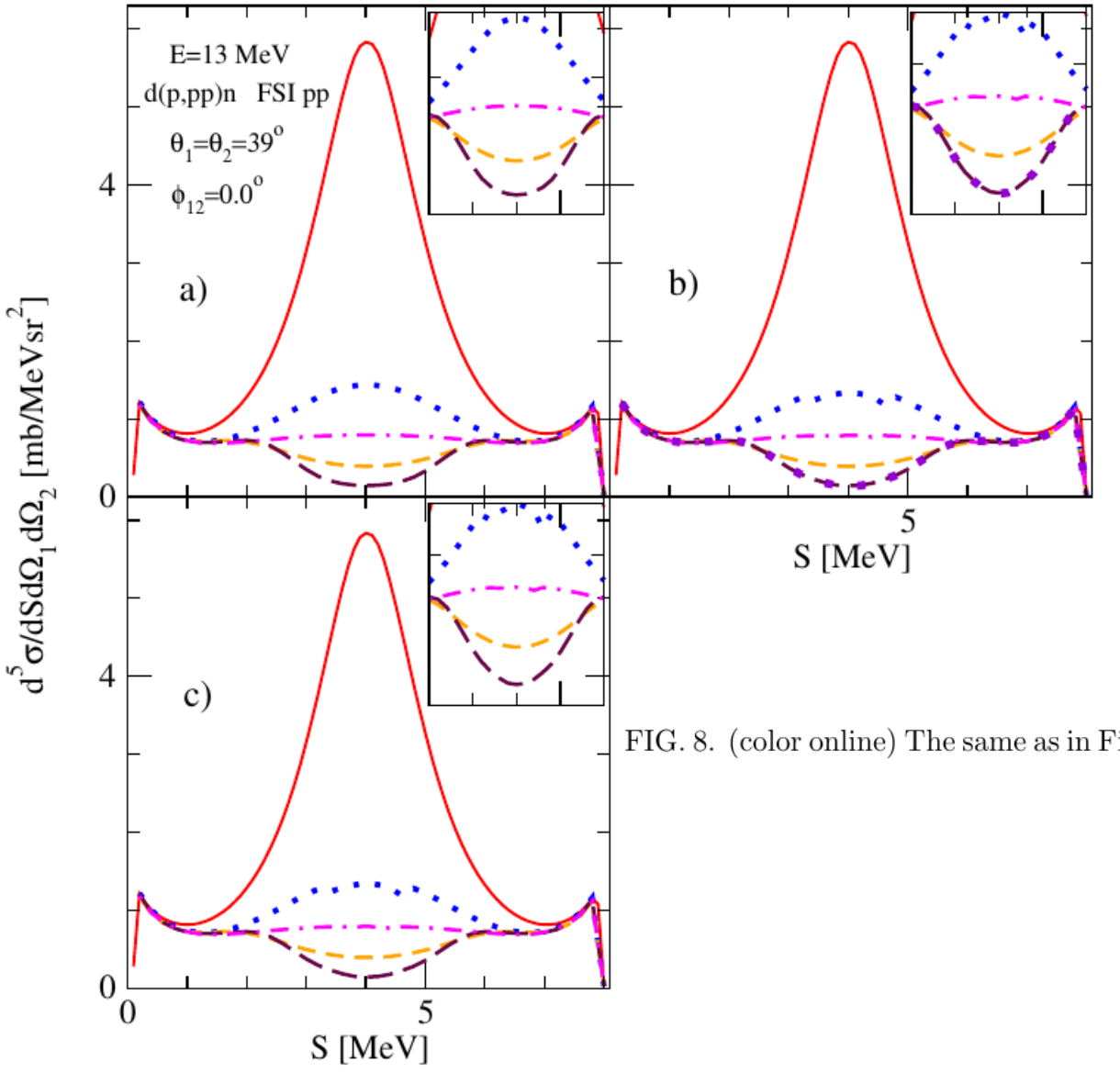

FIG. 8. (color online) The same as in Fig. 7 but for the pp FSI kinematically complete configuration.

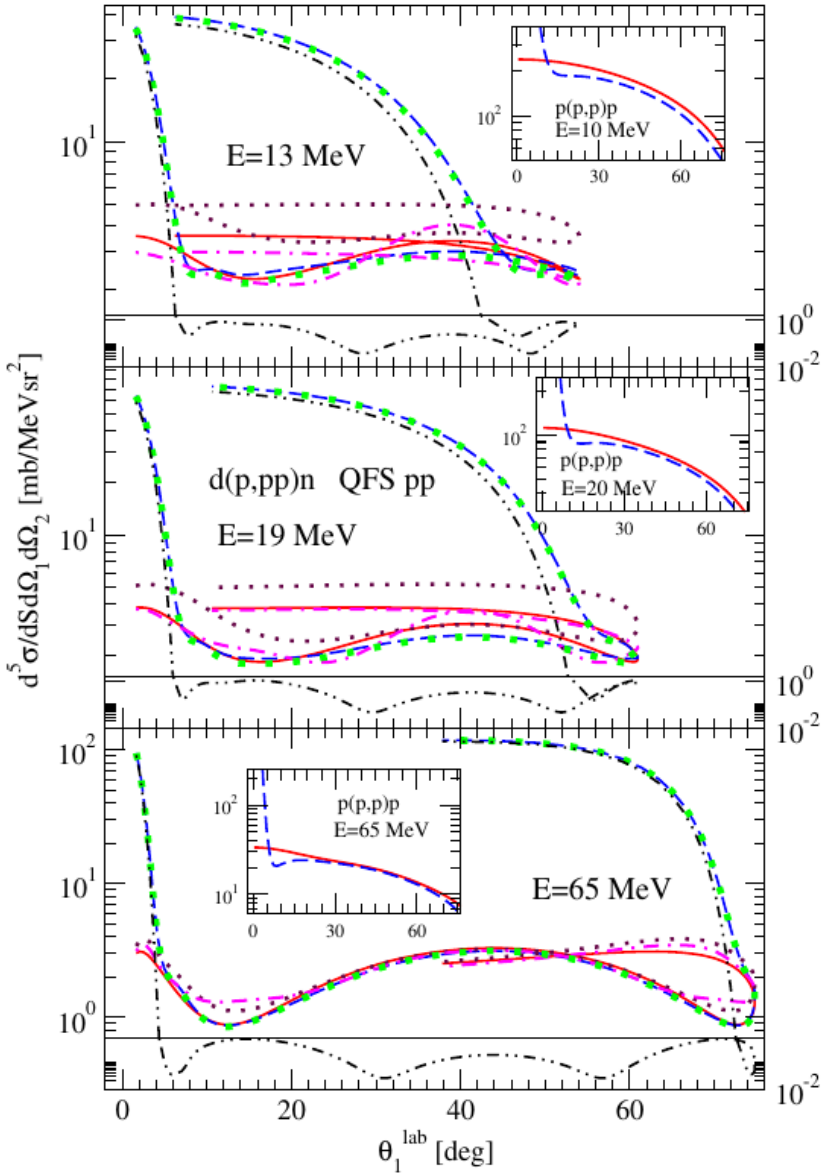

FIG. 9. (color online) The pd breakup d(p,pp)n cross section calculated at the pp QFS condition for the incoming proton lab. energy $E = 13, 19$, and 65 MeV, as a function of the angle of the outgoing proton 1. The approach based on Eq. (12) with set of $js3j3$ partial waves and the screening radius $R = 40$ fm ($n = 4$) was used, with on-shell Faddeev amplitudes obtained by an interpolation from the off-shell ones, renormalized before calculating observables. The blue long-dashed line is the result with all three terms in Eq. (16). Also the result without renormalization is shown by the green dotted line. The maroon dotted and magenta dashed-dotted lines follow when the term with 3-dimensional t_c^R Coulomb t-matrix and both terms with t_c^R are omitted, respectively, and the black double-dotted-dashed line when only these two terms are kept. At bottom of each figure continuation of the black double-dotted-dashed line is shown in a compressed y-axis scale shown on the right side. The red solid line is the nd breakup cross section. In insets the lab. cross sections $d\sigma/d\Omega$ ($\frac{mb}{sr}$) for pp scattering at lab. energies $E = 10, 20$, and 65 MeV are shown as a function of the proton lab. angle. Here the red solid and blue dashed lines are the AV18 cross sections without and with pp Coulomb interaction, respectively.

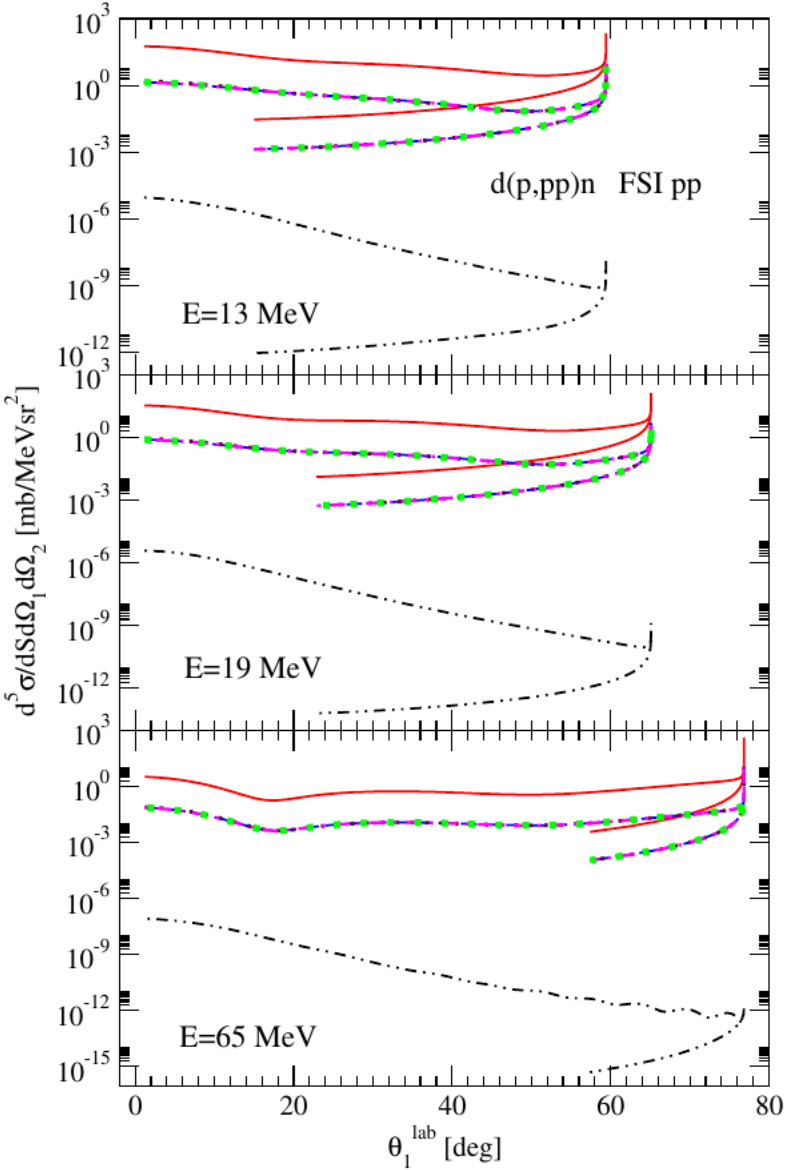

FIG. 10. (color online) The same as in Fig. 9 but for the pd breakup d(p,pp)n cross section $d^5\sigma/d\Omega_1 d\Omega_2 dS$ calculated at the pp FSI condition ($\vec{p}_1 = \vec{p}_2$).

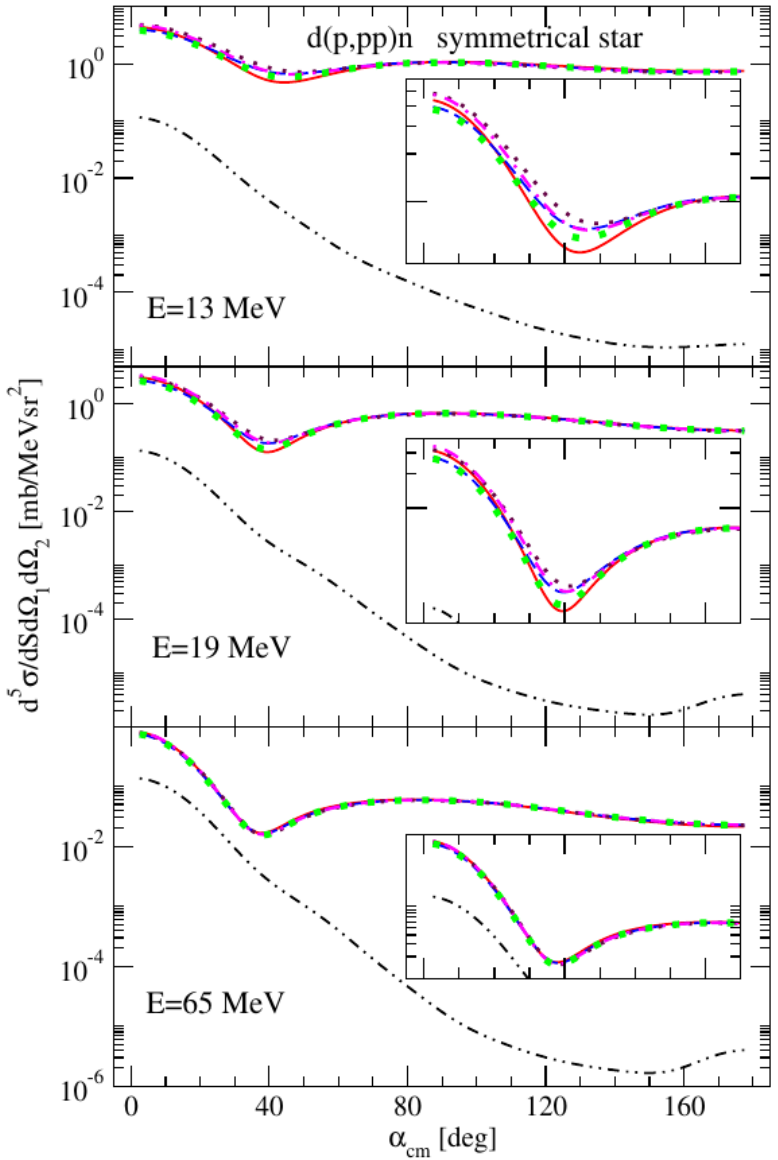

FIG. 11. (color online) The same as in Fig. 9 but for the pd breakup d(p,pp)n cross section $d^5\sigma/d\Omega_1 d\Omega_2 dS$ calculated at the symmetrical-space-star condition (in the 3N c.m. system the momenta of the three outgoing nucleons are equal and form a symmetric three-point star in a plane inclined at an angle α_{cm} with respect to the incoming proton momentum).

Summary:

the two discussed approaches have to provide the same results for all observables

In each method the cancellation between terms containing 3-dimensional and partial wave decomposed Coulomb t-matrices is decisive for establishing workable equations, whose structure is identical to the commonly used equations for neutron-deuteron scattering

Solutions of these equations together with four additional terms, two of which contain the 3-dimensional Coulomb t-matrices, permit one to get the elastic scattering (and breakup) transition amplitudes

In the approach based on the AGS equation it is unavoidable to perform renormalization of the elastic scattering amplitudes before calculating observables

In the approach based on the Faddeev equation such renormalization can be completely avoided

We have shown numerically that the cancellation of last two terms in elastic scattering transition amplitude enables one to determine the pp Coulomb force effects in the pd scattering nearly as easily as to compute observables in neutron-deuteron scattering.

For states $|\alpha>$ with two-nucleon subsystem isospin $t = 1$ the corresponding t-matrix element $< p\alpha|t^R_{N+c}(E - \frac{3}{4m}q^2)|p'\alpha' >$ is a linear combination of the pp, t^R_{pp+c}, and the neutron-proton (np), t_{np}, $t = 1$ t-matrices, which are generated by the interactions $V^{strong}_{pp} + V^R_c$ and V^{strong}_{np}, respectively. The coefficients of that combination depend on the total isospin T and T' of states $|\alpha>$ and $|\alpha'>$ [11, 14]:

$$
\begin{aligned}
&< t = 1T = \frac{1}{2}|t^R_{N+c}|t' = 1T' = \frac{1}{2} > = \frac{1}{3}t_{np} + \frac{2}{3}t^R_{pp+c} \\
&< t = 1T = \frac{3}{2}|t^R_{N+c}|t' = 1T' = \frac{3}{2} > = \frac{2}{3}t_{np} + \frac{1}{3}t^R_{pp+c} \\
&< t = 1T = \frac{1}{2}|t^R_{N+c}|t' = 1T' = \frac{3}{2} > = \frac{\sqrt{2}}{3}(t_{np} - t^R_{pp+c}) \\
&< t = 1T = \frac{3}{2}|t^R_{N+c}|t' = 1T' = \frac{1}{2} > = \frac{\sqrt{2}}{3}(t_{np} - t^R_{pp+c}) \ . \qquad (9)
\end{aligned}
$$

For isospin $t = 0$, where $T = T' = \frac{1}{2}$:

$$
< t = 0T = \frac{1}{2}|t^R_{N+c}|t' = 0T' = \frac{1}{2} > = t_{np} \ . \qquad (10)
$$